

Correlated two-particle scattering on finite cavities

K. Morawetz,^{1,2} M. Schreiber,¹ B. Schmidt,¹ A. Ficker,¹ and P. Lipavský^{3,4}

¹*Institute of Physics, Chemnitz University of Technology, 09107 Chemnitz, Germany*

²*Max-Planck-Institute for the Physics of Complex Systems, Noethnitzer Strasse 38, 01187 Dresden, Germany*

³*Institute of Physics, Academy of Sciences, Cukrovarnická 10, 16253 Prague 6, Czech Republic*

⁴*Faculty of Mathematics and Physics, Charles University, Ke Karlovu 5, 12116 Prague 2, Czech Republic*

(Received 13 September 2004; revised manuscript received 14 December 2004; published 5 July 2005)

The correlated two-particle problem is solved analytically in the presence of a finite cavity. The method is demonstrated here in terms of exactly solvable models for both the cavity as well as the two-particle correlation where the two-particle potential is chosen in separable form. The two-particle phase shift is calculated and compared to the single-particle one. The two-particle bound state behavior is discussed and the influence of the cavity on the binding properties is calculated.

DOI: [10.1103/PhysRevB.72.014301](https://doi.org/10.1103/PhysRevB.72.014301)

PACS number(s): 72.10.Fk, 03.65.Nk, 21.45.+v, 34.10.+x

I. INTRODUCTION

Finite quantum structures are intensively studied concerning their transport properties, trapping behavior, as well as considering them as artificial atoms^{1,2} which become especially interesting in reduced dimensions. The main tool to investigate the properties of such quantum cavities is the scattering of particles connected with excitations³ or the current measurement⁴⁻⁶ through these structures. We want to regard as quantum cavities here also quantum dots or any finite structure. The effort of theoretical investigations has reached a fairly high level adequate to the obtained experimental quality of data. Nevertheless it is noticeable that almost all investigations are restricted to one-particle transport properties like current, conductance, etc. On the other side, the experimental abilities are on such a level that also higher-order correlations and more than one-particle properties can be envisaged. The aim of the present paper is to investigate two-particle correlations together with one-particle correlations on the same footing. Since these investigations suggest looking at a new type of experiment on quantum cavities we want to present an exactly solvable model for exploratory reasons. In this way the method is demonstrated which can then be used for any realistic nanostructure, with an amorphous or crystalline system as background provided the one-particle wave functions are available from, e.g., standard *ab initio* methods.

As illustrated in Fig. 1, we consider the gedanken experiment to scatter two particles with each other in the presence of a quantum cavity. In usual approaches it would be sufficient to know the scattering properties of single particles (though correlated) on the cavity in order to describe the transport properties. We want to demonstrate that the two-particle correlations in addition to the scattering on the quantum cavity lead to interesting effects of coupled channels which might be worth an experimental investigation.

As sketched by the figure, we face a two-center scattering which is conveniently described by coupled-channel scattering theory.⁷ A similar problem has been considered by Beregi *et al.*,⁸ Beregi and Lovas,⁹ and Beregi¹⁰ who solved the problem with the help of the Faddeev technique. We will adopt here a simpler approach which is possible due to the Gell-

Mann and Goldberger formulation.¹¹ Due to the different occurring interactions, we define two channels, the one-particle scattering channel $V_1 = V_a + V_b$ and the corresponding two-particle one $V_2 = V_{ab}$. The total \mathcal{T} matrix can be found by the Gell-Mann and Goldberger two-potential formula¹¹ summarized in Appendix A

$$\mathcal{T} = \mathcal{T}_1 + (1 + V_1 \mathcal{G}_1) \mathcal{T}_{ab} (1 + \mathcal{G}_1 V_1). \quad (1)$$

Here the one-particle \mathcal{T} matrix is given by

$$\mathcal{T}_1 = V_1 + V_1 \mathcal{G}_1 V_1 \quad (2)$$

and the correlated two-particle \mathcal{T} matrix \mathcal{T}_{ab} is a solution of the modified Lippmann-Schwinger equation

$$\mathcal{T}_{ab} = V_2 + V_2 \mathcal{G}_1 \mathcal{T}_{ab}, \quad (3)$$

where the full solution of the one-particle channel enters in \mathcal{G}_1 . For that one assumes that the one-particle problem is solved and the propagator in the one-particle channel is known $\mathcal{G}_1 = (\omega - \mathcal{H}_1)^{-1}$. This scheme is advisable if one channel can be solved exactly and the other channel is then described by a Lippmann-Schwinger Eq. (3) with the help of the solved channel. This method has been compared to other coupled-channel methods¹² and successfully applied to defects in potentials¹³ and in developing a hybrid representation of the nuclear potential.¹⁴ We will use this scheme here and will employ an exactly solvable model for both channels.

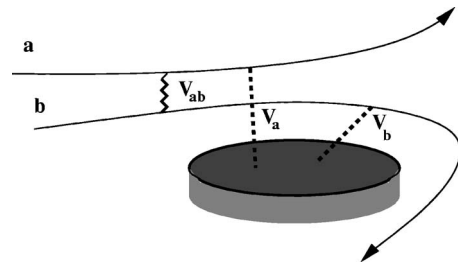


FIG. 1. Schematic picture of correlated two-particle scattering on a quantum cavity.

II. MODEL

A. Model cavity

For the cavity we choose a model of an opaque wall in three dimensions which can be found in text books.¹⁵ This model is able to simulate properties of opaque confining traps as well as parametric resonances. The potential in the single-particle channel takes the form

$$V_a(r) = \frac{1}{2m} \frac{\Omega}{R} \delta(r-R) \quad (4)$$

with the reduced mass m of particles a and b scaled out. Thus we have an opaque delta potential at the radial distance $r=R$ from the center of the cavity. The wave functions outside and inside the cavity decouple completely in the limit of hard spheres $\Omega \rightarrow \infty$, where the interior of the cavity is characterized by discrete energy levels. For the opaque wall, $\Omega < \infty$, outside and inside are coupled and resonances occur at the virtual levels.

The wave function of this radial problem has the form $\Psi_n(r) = \langle r|n \rangle = \chi_n(r)/r$. While the subscript n denotes general quantum numbers the specific wave function here shall be characterized by continuous momenta $n=k$ such that

$$\chi_k(r) = c \begin{cases} A_{kR} \sin kr; & r < R \\ \sin(kr + \phi); & r > R \end{cases} \quad (5)$$

The one-particle phase shift ϕ is determined by

$$\cot(x + \phi) - \cot x = \Omega/x, \quad (6)$$

where $x=kR$. The amplitude can be written as

$$A_x^2 = \frac{\sin^2(x + \phi)}{\sin^2 x} = \frac{1 + \tan^2 x}{\tan^2 x + \left(1 + \frac{\Omega}{x} \tan x\right)^2} \quad (7)$$

and shows resonances at the virtual levels

$$\tan 2x_\nu = -2x_\nu/\Omega, \quad (8)$$

with even ν which approaches the levels $x_\nu = k_\nu R = \nu\pi$ in case of an impenetrable wall, $\Omega \rightarrow \infty$. Assuming only s-wave scattering the corresponding single-particle cross section reads

$$\sigma(k) = \frac{4\pi}{k^2} \frac{1}{1 + \cot^2 \phi}, \quad (9)$$

which has zeros at $x_n = n\pi$. From Eq. (6) one finds that the cross section has a limited number of maxima at

$$-2 \frac{x_\mu}{\Omega} = \sin 2x_\mu \quad (10)$$

depending on the potential strength $\Omega - \pi/2 \geq 2\pi|\mu|$. These maxima are accompanied by minima and an infinite number of further maxima at

$$-2 \frac{x_\mu}{\Omega} = \tan 2x_\mu. \quad (11)$$

These features are illustrated in Fig. 2.

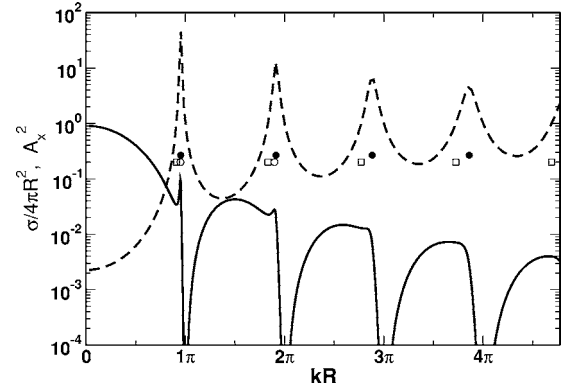


FIG. 2. Single-particle cross section on the cavity (9) with zeros at $kR=n\pi$ (solid line) and the amplitude (7) versus momenta for $\Omega=20$. The filled circles marks the maxima of the amplitude (8), the open circles the maxima of the cross section according to Eq. (10) and the open squares the minima and maxima of the cross section according to Eq. (11).

B. Two-particle problem with separable potential

We study in this paper the combined problem of single- and two-particle scattering and will use a separable representation of the two-particle interaction which provides tremendous technical simplifications. One can show that the effect of any finite-range potential on the scattering wave function Ψ can be represented in separable form^{16,17}

$$\mathcal{V}|\psi\rangle = \sum_{ij} |g_i\rangle \tau_{ij} \langle g_j|p\rangle, \quad (12)$$

where $|p\rangle$ is the undisturbed plane wave and g_i are form factors. This is known as the expansion of the wave function inside the potential range and outlined in Appendix B. Separable potentials are powerful tools for constructing unknown nuclear matter potentials from available experimental scattering phase shifts by inverse scattering theory.¹⁸ The application of such separable potentials is versatile ranging from plasma physics¹⁹ to medium modification of transport properties in nuclear matter²⁰⁻²² up to high field problems in superconductivity.²³

According to the Gell-Mann and Goldberger formula (1) we assume the one-particle wave function $|n_1\rangle$ to be known

$$\mathcal{H}_1|n_1\rangle = E_{n_1}|n_1\rangle. \quad (13)$$

The two-particle \mathcal{T} matrix Eq. (3) is now represented in momentum states. We note the momentum difference of the two particles by small letters, e.g., p , and the center-of-mass momentum by capital letters, e.g., P . Introducing a complete set $|n_1 n_2\rangle$ according to Eq. (13) we obtain

$$\begin{aligned} \langle p_1 P | \mathcal{T}_{ab} | p_2 P' \rangle &= V_{p_1 p_2} \delta_{PP'} + \sum_{n_1 n_2 p' \bar{p}} \\ &\times V_{p_1 p} \frac{\langle p P | n_1 n_2 \rangle \langle n_1 n_2 | p' \bar{p} \rangle}{\omega - E_{n_1 n_2} + i\eta} \langle p' \bar{p} | \mathcal{T}_{ab} | p_2 P' \rangle. \end{aligned} \quad (14)$$

By convention we use $\Sigma_q = \int d\mathbf{q} / (2\pi)^3$ and set $\hbar=1$ within

this paper. Equation (14) is the exact formulation of the quantum two-particle problem in channel 2. It can be solved with the help of such a separable potential²⁴

$$V_{pq} = \lambda g_p g_q \quad (15)$$

with form factors g_p as given in Appendix C. While generally any finite-range potential can be represented in a separable form of finite rank, we restrict ourselves here to rank-one potentials for exploratory reasons. The technique remains the same for high-rank potentials.

III. TWO-PARTICLE SCATTERING ON FINITE CAVITY

A. Free two-particle problem

The case without cavity or unrestricted two-particle scattering is solved by plane waves with the center-of-mass momentum K and the difference momentum k as good quantum numbers $|n_1 n_2\rangle = |kK\rangle$. Performing the k, K integrations, the Lippmann-Schwinger Eq. (14) reads with $\langle p_1 P | \mathcal{T}_{ab} | p_2 P' \rangle = \delta_{PP'} t_{p_1 p_2}(P)$

$$t_{p_1 p_2}(P) = \lambda g_{p_1} g_{p_2} + \lambda \sum_q g_{p_1} g_q \frac{t_{qp_2}}{\omega - \frac{P^2}{4m} - \frac{q^2}{m} + i\eta}, \quad (16)$$

which is easily solved as

$$t_{p_1 p_2}(P) = \frac{\lambda g_{p_1} g_{p_2}}{1 - \lambda J(P, \omega)},$$

$$J(P, \omega) = \sum_q \frac{g_q^2}{\omega - \frac{P^2}{4m} - \frac{q^2}{m} + i\eta}. \quad (17)$$

This result is given explicitly for different form factors in Appendix C.

B. Two-particle scattering and cavity

Now we are going to consider the disturbed two-particle scattering problem, which should reduce to Eq. (17) in the limit of unrestricted two-particle scattering. The equation for the \mathcal{T} -matrix (14) can be simplified by introducing the modified form factors

$$G_{n_1 n_2}(P) = \sum_p g_p \langle pP | n_1 n_2 \rangle. \quad (18)$$

Splitting off the trivial factors

$$\langle p_1 P | \mathcal{T}_{ab} | p_2 P' \rangle = \lambda g_{p_1} g_{p_2} t(PP'), \quad (19)$$

from Eq. (14) the equation for the center-of-mass dependence follows

$$t(PP') = \delta_{PP'} + \lambda \sum_{n_1 n_2} \frac{G_{n_1 n_2}(P) \sum_{\bar{P}} G_{n_1 n_2}^*(\bar{P}) t(\bar{P}P')}{\omega - E_{n_1 n_2} + i\eta}. \quad (20)$$

The completeness of $|n_1 n_2\rangle$ implies the relation

$$\sum_{n_1 n_2} G_{n_1 n_2}(P) G_{n_1 n_2}^*(P') = \delta_{PP'} \sum_q g_q^2. \quad (21)$$

We introduce the auxiliary function

$$h_{n_1 n_2}^*(P') = \sum_{\bar{P}} G_{n_1 n_2}^*(\bar{P}) t(\bar{P}P') \quad (22)$$

from which the \mathcal{T} matrix can be obtained with the help of Eq. (21) as

$$t(PP') = \frac{1}{\sum_q g_q^2} \sum_{n_1 n_2} G_{n_1 n_2}(P) h_{n_1 n_2}^*(P'). \quad (23)$$

Multiplying Eq. (20) with $G_{m_1 m_2}^*(P)$ and integrating over P we obtain an equation for the auxiliary function (22)

$$h_{m_1 m_2}^*(P') = G_{m_1 m_2}^*(P') + \sum_{n_1 n_2} H_{m_1 m_2 n_1 n_2} h_{n_1 n_2}^*(P') \quad (24)$$

with

$$H_{m_1 m_2 n_1 n_2} = \lambda \frac{\sum_P G_{m_1 m_2}^*(P) G_{n_1 n_2}(P)}{\omega - E_{n_1 n_2} + i\eta}. \quad (25)$$

For cavities possessing only discrete states in which case n_i and m_i are natural numbers, Eq. (24) is a linear equation system which can be easily solved. With the help of Eqs. (23) and (19) the \mathcal{T} matrix is consequently found exactly.

The situation becomes more complicated if continuum states are present in the cavity. Then the quantum numbers $\langle n_1 n_2 |$ become continuous variables like in the case of the free two-particle problem and Eq. (24) turns into an integral equation. We cannot present at the moment the analytical exact solution of the combined problem consisting of bound and scattering states. The numerical scheme consists in discretizing this continuous integral and solving the linear equation system (24). This complete numerical solution will be devoted to a forthcoming work. To get a first physical insight, we will instead restrict ourselves in this paper only to cavities with no bound states, i.e., only scattering states, and moreover to scattering events where the center-of-mass momenta of the two particles are not remarkably changed.

C. Approximated solution

Due to the spatial structure of the one-particle problem, in general we will not have translational symmetry. This means that the two-particle problem need not have the same center-of-mass momenta of incoming and outgoing particles. Only in special cases like the zero center-of-mass momentum and no change of the total momentum due to release or capturing of momentum by the cavity, we can assume approximately a diagonal form $t(PP') \approx \delta_{PP'} t(P)$.

We understand this approximation as considering the effect of the cavity on the free two-particle problems (16) and (17) in first order. Such a diagonal solution is obtained, if for the momentum integral over \bar{P} on the right-hand side of Eq. (20) we apply the mean value theorem of integrals and approximate the mean value \bar{P} by the center-of-mass momentum P

$$\begin{aligned} \sum_{\bar{P}} G_{n_1 n_2}^*(\bar{P}) t(\bar{P} P') &= t(\bar{P} P') \sum_{\bar{P}} G_{n_1 n_2}^*(\bar{P}) \\ &\approx t(P P') \sum_{\bar{P}} G_{n_1 n_2}^*(\bar{P}). \end{aligned} \quad (26)$$

Then Eq. (20) is easily solved and the diagonal \mathcal{T} matrix is

$$\langle p_1 P | \mathcal{T}_{ab} | p_2 P' \rangle = \delta_{PP'} \frac{\lambda g_{p_1} g_{p_2}}{1 - \lambda J(P, \omega)} \quad (27)$$

with

$$J(P', \omega) = \sum_{n_1 n_2} \frac{\sum_P G_{n_1 n_2}(P) G_{n_1 n_2}^*(P')}{\omega - E_{n_1 n_2} + i\eta}. \quad (28)$$

Alternatively we can obtain this result by assuming *ad hoc* a diagonal \mathcal{T} matrix $t(P P') \approx \delta_{PP'} t(P)$ which according to Eq. (20) fulfills the integral equation

$$t(P') \delta_{PP'} = \delta_{PP'} + \lambda \sum_{n_1 n_2} \frac{G_{n_1 n_2}(P) \sum_{\bar{P}} G_{n_1 n_2}^*(\bar{P}) t(P') \delta_{P\bar{P}'}}{\omega - E_{n_1 n_2} + i\eta}. \quad (29)$$

Integrating this equation over P we obtain the same approximate solution (27)

$$t(P') = \frac{1}{1 - \lambda J(P', \omega)}. \quad (30)$$

It is interesting to note here that Eq. (30) is also a solution of a nontrivial integral equation. To see this one can integrate Eq. (29) over P' instead of over P as done above. One then obtains the integral equation

$$t(P) = 1 + \lambda \sum_{n_1 n_2} \frac{G_{n_1 n_2}(P) \sum_{\bar{P}} G_{n_1 n_2}^*(\bar{P}) t(\bar{P})}{\omega - E_{n_1 n_2} + i\eta}. \quad (31)$$

Therefore we can conclude that Eq. (30) is also an approximate diagonal solution of the integral Eq. (31) which has not been known previously to the authors' knowledge.

The approximate solution (27) together with Eqs. (28) and (18) is the main result which we will employ within this paper. It represents a generalization of the standard separable \mathcal{T} matrix result, e.g., of Ref. 24, in two respects: (i) It describes the two-particle scattering on a finite cavity or on an arbitrary structure represented by the one-particle wave functions and (ii) it gives the exact solution of the two-particle quantum problem in the case of conservation of total momentum before and after scattering.

Before continuing we want to show first how the limit of unrestricted two-particle scattering is reached. Unrestricted scattering means the absence of the cavity so that the single-particle wave functions become plane waves $|n_1 n_2\rangle = |kK\rangle$ as discussed in Sec. III A. Consequently, Eq. (18) takes the form

$$G_{kK}^{\text{inf}}(P) = g_k \delta_{PK} \quad (32)$$

and Eq. (28) is

$$J^{\text{inf}}(P\omega) = \sum_q g_q^2 \frac{1}{\omega - E_{P/2+q} - E_{P/2-q} + i\eta}, \quad (33)$$

which is the standard expression for unrestricted two-particle scattering (17) and separable interaction. In nuclear physics this case is labeled infinite matter.

IV. ANALYTICAL RESULTS FOR TWO-PARTICLE SCATTERING ON AN OPAQUE WALL

We are now going to evaluate the result (27) with Eqs. (28) and (18). Restricting the calculation to a rank-one separable potential characterized by only one form factor, e.g., $g_p = \exp(-p^2/4\beta^2)/\beta^2$, and the potential strength λ , one can describe two properties of the two-particle correlations, the scattering length a_0 and the range of the potential r_0 as illustrated in Appendix C. For clarity we will first concentrate only on the scattering length and will separate the effects of potential range. Therefore it is advisable to start with the contact potential which is represented by the limit of zero range $\beta \rightarrow \infty$. In a second step we will discuss the effects of finite range of the potential.

A. Contact potential for two-particle correlations

The separable potential allows us to adopt the contact potential by a special limit using a parameter-dependent coupling constant $\lambda(\beta)$ such that the scattering length is kept fixed. In this way one ensures intrinsically the necessary renormalizations which otherwise have to be performed by subtracting diverging terms to fix the scattering length to the physical value.²⁵

Mathematically, the limit $\beta \rightarrow \infty$ with fixed scattering length is realized if we rewrite the coupling constant λ in terms of the scattering length. This is obtained from the general relation between phase shift φ and the \mathcal{T} matrix

$$\tan \varphi = \frac{\text{Im } T}{\text{Re } T} \Big|_{\omega=p^2/m}; \tan \varphi^{\text{inf}} = \frac{\lambda J_1^{\text{inf}}}{1 - \lambda J_R^{\text{inf}}}, \quad (34)$$

where we will abbreviate the real and imaginary parts of the unrestricted two-particle scattering expression (33) as $J_R^{\text{inf}} = \text{Re } J^{\text{inf}}(P, p^2/m)$ and $J_1^{\text{inf}} = \text{Im } J^{\text{inf}}(P, p^2/m)$, respectively. One knows that for contact potentials²⁶

$$\tan \varphi^{\text{inf}} = p a_0 \quad (35)$$

for all momenta p and we express the parameter-dependent coupling constant $\lambda(\beta)$ from Eq. (34) as

$$\lambda = \frac{p a_0}{J_1^{\text{inf}} + p a_0 J_R^{\text{inf}}}. \quad (36)$$

Inserting this expression into Eq. (27) we obtain

$$\mathcal{T}_{ab}(P, \omega) = \frac{\lambda g_{p_1} g_{p_2}}{1 - \lambda J(P, \omega)} = \frac{p a_0 g_{p_1} g_{p_2}}{J_1^{\text{inf}} - p a_0 [J_R^{\text{inf}} - J(P, \omega)]}. \quad (37)$$

Now we are ready to perform the limit of zero range $\beta \rightarrow \infty$. From Eqs. (28) and (33) one sees that the form factors

$g_p=1/(\beta^2+p^2)$ appear with the same order in the numerator as well as in the denominator which cancel in the limit of zero range. Consequently, Eq. (37) for the \mathcal{T} matrix (27) approaches

$$\mathcal{T}_{ab}(P, \omega) \rightarrow \mathcal{T}_{ab}^0(P, \omega) = \frac{pa_0}{J_1^{0\text{inf}} - pa_0[J_R^{0\text{inf}} - J^0(P, \omega)]}, \quad (38)$$

where the additional superscript 0 denotes that both expressions (28) and (33) have to be taken with $g_p \rightarrow 1$. The difference $J_R^{0\text{inf}} - J^0$ in the denominator (38) ensures the convergence of the expression since $\text{Re } J$ and $J_R^{0\text{inf}}$ diverge.

It is instructive to check the \mathcal{T} matrix for contact potentials without cavity. From Eq. (33) one has

$$J_1^{0\text{inf}}\left(P, \omega + \frac{P^2}{4m}\right) = -\frac{m}{4\pi} \sqrt{m\omega} \Theta(\omega),$$

$$J_R^{0\text{inf}}\left(P, \omega + \frac{P^2}{4m}\right) = \frac{1}{2\pi^2} \int_0^\infty \frac{dkk^2}{\omega - \frac{k^2}{m}}, \quad (39)$$

which leads to the \mathcal{T} matrix (38) for contact potentials in unrestricted two-particle scattering

$$\frac{1}{\mathcal{T}^{0\text{inf}}\left(P, \omega + \frac{P^2}{4m}\right)} = \frac{m}{4\pi} \begin{cases} -\frac{1}{a_0} + ip; & \omega = \frac{p^2}{m} \\ -\frac{1}{a_0} - \sqrt{mE_b}; & \omega = -E_b \end{cases}. \quad (40)$$

Though Eq. (39) diverges, the solution (38) remains finite. With the help of Eq. (34) one can convince oneself that Eq. (35) is fulfilled for positive energies $\omega=p^2/m$ as it should be²⁷ and that in the case where the scattering length is negative indicating attraction, the bound state $E_b=1/ma_0^2$ represents the pole of the \mathcal{T} matrix at $\omega=-E_b$.

Now we are going to calculate J^0 according to Eq. (28) including the finite cavity represented by the single-particle wave function $|n\rangle$ in Eq. (5). The explicit form for Eq. (18) reads

$$G_{n_1 n_2}^0(P) = \sum_p \langle pP | n_1 n_2 \rangle = \int d\mathbf{r} e^{-i\mathbf{r}\cdot\mathbf{P}} \Psi_{n_1}(\mathbf{r}) \Psi_{n_2}(\mathbf{r}), \quad (41)$$

where the spatial representation of the one-particle wave function is $\Psi_{n_1}(\mathbf{r}) = \langle \mathbf{r} | n_1 \rangle$. This means that

$$\sum_P G_{n_1 n_2}^0(P) = \Psi_{n_1}(0) \Psi_{n_2}(0),$$

$$G_{n_1 n_2}^0(0) = \sqrt{2} \delta_{n_1 n_2}. \quad (42)$$

The last equality follows from the completeness of the set of single-particle wave functions as well as the normalization

$$\int d\mathbf{r} |\Psi_{n_1}|^2 = \sqrt{2} \quad (43)$$

ensuring that the normalization of the wave function $|n_1 n_2\rangle$ is 2 for the two particles.

Now we can give a simple expression for Eq. (28) in the case of center-of-mass scattering $P=0$ which we want to discuss in the following. We obtain with the help of Eq. (42)

$$J^0(0, \omega) = \sum_{n_1} \frac{|\Psi_{n_1}(0)|^2 \sqrt{2}}{\omega - 2E_{n_1} + i\eta}. \quad (44)$$

Together with Eq. (39) we have obtained the two-particle \mathcal{T} matrix for contact interaction (38) provided the one-particle wave function of the cavity $\Psi_{n_1}(r) = \langle r | n_1 \rangle = \chi_{n_1}(r)/r$ and the single-particle energy E_{n_1} according to Eq. (13) are known. For this purpose we use Eq. (5) of the opaque wall and the necessary part of the wave function in Eq. (44) reads

$$\Psi_{n_1}(0) = ckA_{kR} \quad (45)$$

with the amplitude given by Eq. (7). We determine the normalization c in such a way that the particle should be in a sphere with radius L which is set to infinity in the end. For such large boundaries we can employ radial cyclic boundary conditions $\chi(r+L) = \chi(r)$, such that we have

$$\sum_{n_1} = \frac{L}{2\pi} \int_0^\infty dk. \quad (46)$$

Calculating the norm (43) with Eq. (5) it follows that

$$\lim_{L \rightarrow \infty} \frac{Lc^2}{2\pi} = \frac{\sqrt{2}}{4\pi^2}. \quad (47)$$

Therefore, the arbitrary large fictitious boundary length L is dropping out in Eq. (44) and we obtain

$$\text{Re } J^0(0, \omega) = \frac{1}{2\pi^2} \int_0^\infty dk \frac{k^2 A_{kR}^2}{\omega - \frac{k^2}{m}}$$

$$\text{Im } J^0\left(0, \omega = \frac{p^2}{m}\right) = -\frac{mp}{4\pi} A_{pR}^2. \quad (48)$$

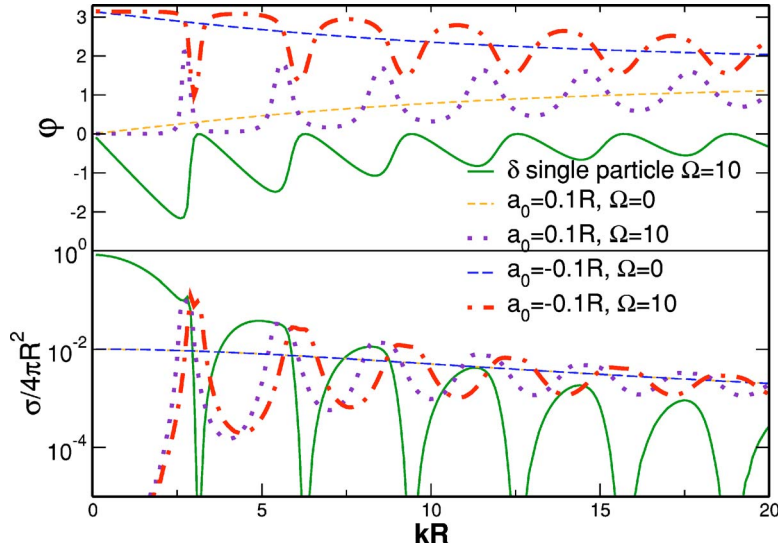
This allows us to determine the \mathcal{T} matrix (38) with the help of Eq. (39) as

$$\frac{m}{4\pi a_0} \mathcal{T}_{ab}^0\left(0, \frac{p^2}{m}\right) = \left(-1 - \frac{a_0}{R} F_\Omega(pR) + ipa_0 A_{pR}^2\right)^{-1} \quad (49)$$

with

$$F_\Omega(z) = \frac{2}{\pi} \int_0^\infty dx \frac{x^2}{z^2 - x^2} (A_x^2 - 1). \quad (50)$$

Please note that the -1 term comes from the subtraction of Eq. (39) in Eq. (38) which renders the expression finite. The function F can be given analytically as presented in Appendix D. From Eqs. (49) and (34) we obtain the two-particle phase shift



$$\tan \varphi(p) = \frac{pRA_{pR}^2}{F_{\Omega}(pR) + \frac{R}{a_0}}. \quad (51)$$

In Fig. 3 we plot the phase shifts for a repulsive opaque wall with $\Omega=10$ and a weak two-particle scattering length of $a_0 = \pm 0.1R$. The one-particle phase shift ϕ is negative indicating repulsion and has the typical oscillatory structure¹⁵ due to the resonances at the virtual levels. The free two-particle phase shift φ^{inf} of Eq. (35) approaches $\pi/2$ for large k and starts from zero for positive a_0 and from π for negative scattering length indicating a bound state according to the Levinson theorem,²⁸ and even numbers to positive scattering lengths. The two-particle phase shift (51) for the case including the opaque wall follows the free two-particle scattering case for such small scattering lengths though the oscillations of the one-particle problem are visible. Interestingly these oscillations are shifted slightly when positive and negative scattering lengths are compared.

With the help of Eq. (51) the corresponding cross section takes the form

$$\sigma = \frac{4\pi}{p^2} \sin^2 \varphi = 4\pi R^2 \frac{A_x^4}{x^2 A_x^4 + \left[F_{\Omega}(x) + \frac{R}{a_0} \right]^2} \quad (52)$$

which will be determined by the structure of the one-particle amplitude A and a combination of A and F dependent on a_0 in the denominator of Eq. (52). The latter leads to additional structure in the cross section and can be understood as an interference between the one-particle and two-particle properties. This can barely be recognized in Fig. 3 where a second maximum appears besides the oscillations given by the one-particle cross section. The appearance of this second maximum is much more pronounced when we go to larger scattering lengths corresponding to stronger two-particle correlation as in Fig. 4. Therefore, it is a correlation effect in the two-particle channel.

Figure 4 also shows that the two-particle problem in the presence of a cavity has no bound state anymore though the free two-particle problem has one. The repulsive opaque wall has destroyed the bound state formation. In order to understand this behavior we consider the \mathcal{T} matrix not at positive

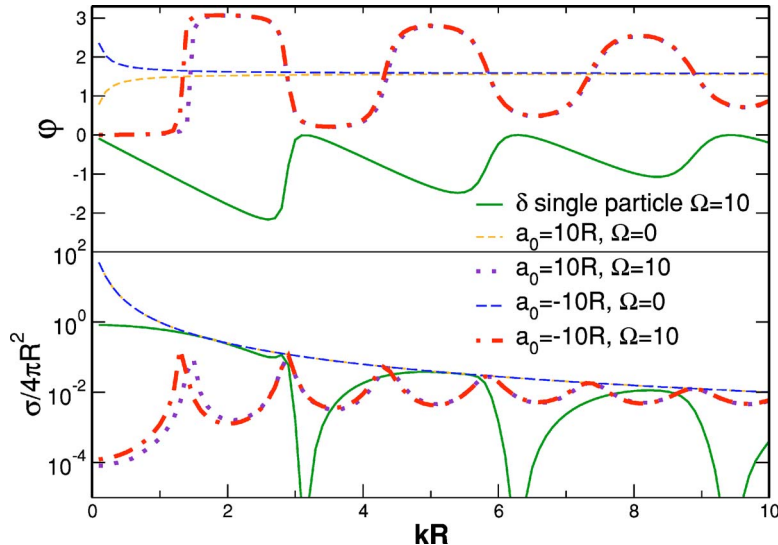


FIG. 4. (Color online) Same as Fig. 3 but for $a_0 = \pm 10R$.

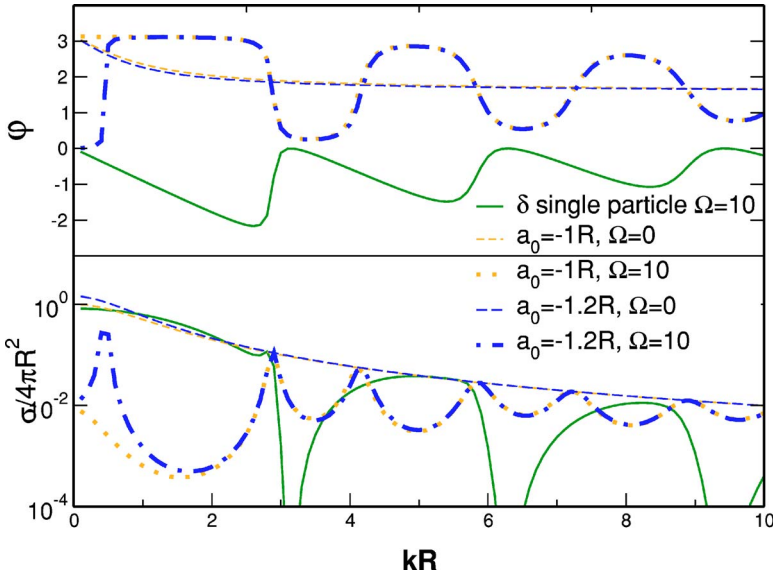


FIG. 5. (Color online) Same as Fig. 3 but for $a_0=-1.2R$ and $a_0=-R$.

energies $\omega=k^2/m$ as done so far but at negative energies where the pole yields the bound state energy $\omega=-E_b$. The \mathcal{T} -matrix (38) reads in this case

$$\mathcal{T}_{ab}^0(0, -E_b) = \frac{-4\pi a_0/m}{1 + a_0\sqrt{mE_b} + \frac{a_0}{R}F_\Omega(iR\sqrt{mE_b})} \quad (53)$$

with F from Eq. (50). Consequently, the bound state energies are given by the pole

$$-\frac{R}{a_0} = F_\Omega(ib) + b \quad (54)$$

with $b=R\sqrt{mE_b}$. It is easy to prove that $F_\Omega(ib)+b \geq F_\Omega(0)$, the explicit analytical expression can be found in Appendix D. This means, as soon as the cavity parameter Ω , R , and the two-particle scattering length a_0 fulfill the inequality

$$-\frac{R}{a_0} \geq F_\Omega(0) \quad (55)$$

we will have two-particle bound states. In Fig. 3 this is the case for negative scattering lengths since $R/a_0=-10$ and $F_{10}(0)=10/11$ while no bound states occur for positive scattering length $R/a_0=10$. Oppositely, in Fig. 4 for both positive and negative scattering lengths we have $R/a_0=\pm 0.1 < F_{10}(0)=10/11$ and no bound states appear anymore. In this figure the free two-particle problem has a bound state for negative scattering length while the repulsive wall allows no bound state for these parameters. According to Eq. (55) the limiting scattering length is $a_0=-1.1R$ for $\Omega=10$. In Fig. 5 we plot the cases just slightly above and below that critical value. One sees that the bound state present in the free case is destroyed by the cavity if the scattering length is more negative than the lower critical value.

It is now interesting to consider the attractive wall $\Omega < 0$. Then we might expect that bound states are favored in any case which is surprisingly not true.

We plot the function $F_\Omega(0)$ in Fig. 6. In the range $\Omega_1 < \Omega < 0$, $F_\Omega(0)$ becomes negative. Therefore any negative a_0 leads to a bound state according to Eq. (55). Both two-particle scattering as well as the opaque wall are attractive and also their combination acts attractively. Positive a_0 will lead to a bound state if $a_0 \geq -R/F_\Omega(0) \geq 0$. Though the wall is attractive to both particles, bound states occur only if the two-particle correlations are larger than a critical value.

This is illustrated in Fig. 7. In this figure we have chosen free two-particle scattering parameters which do not lead to bound states. The attractive opaque wall creates a bound state for $a_0=0.5R$ while no bound state occurs for $a_0=0.25R$.

For the range $\Omega < \Omega_1$ the function $F_\Omega(0)$ is positive. This means that the same discussion holds as for positive Ω . According to Eq. (55) a_0 must be negative and $a_0 \geq -R/F_\Omega(0)$. This means that bound states occur only if the two-particle scattering length is larger than a critical value. The appearance of such critical values for the two-particle scattering

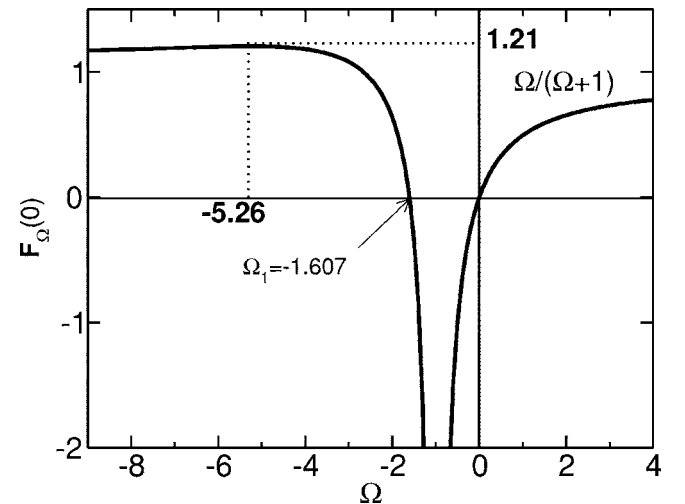


FIG. 6. Function $F_\Omega(0)$ of Eq. (50) which allows bound states if $-R/a_0 \geq F_\Omega(0)$ according to Eq. (55).

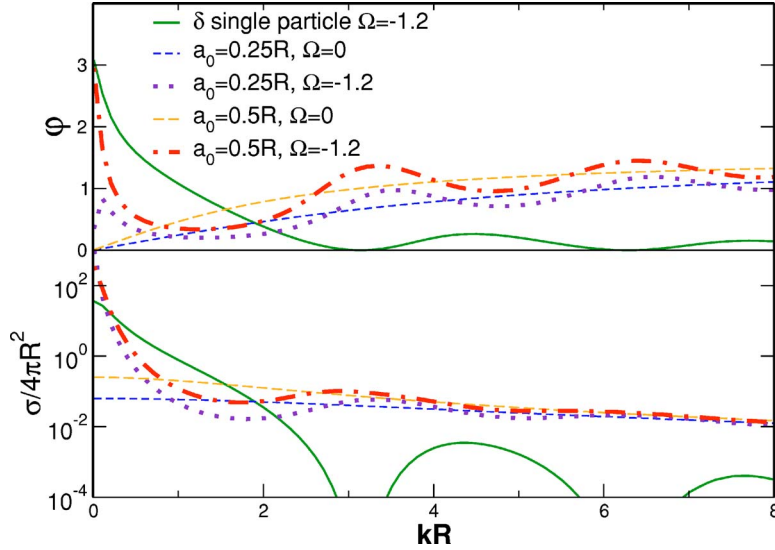


FIG. 7. (Color online) Same as Fig. 3 but with $\Omega = -1.2$ which corresponds to $F_\Omega(0) = -3.33$ and $a_0 = 0.25R$ and $a_0 = 0.5R$.

length is an unexpected effect of interference. Please note also that if $1 \leq F_\Omega(0) \leq 1.21$ there are two values of Ω which lead to the same $F_\Omega(0)$. This means we can have two different cavities Ω which yield the same bound state.

B. Finite range effects

After discussing the effect of the scattering length we want to return to the more realistic situation of finite-range two-particle interaction. Therefore we choose a separable form of the potential and evaluate Eq. (28) explicitly. For exploratory reasons we choose the exponential form factor of Appendix C 1 and the center-of-mass system $P=0$.

Introducing the dimensionless integrals

$$G_{n_1 n_2}(0) = \int \frac{d\mathbf{q}}{(2\pi)^3} g_q \Psi_{\mathbf{k}_1}(\mathbf{q}) \Psi_{\mathbf{k}_2}(-\mathbf{q}) \equiv \frac{8Rc^2}{\beta^2} \tilde{G}_0(x_1, x_2)$$

$$\int \frac{d\mathbf{p}}{(2\pi)^3} G_{n_1 n_2}(p) = \frac{32\beta R c^2}{\sqrt{\pi}} \bar{G}(x_1, x_2) \quad (56)$$

with $x_n = Rk_n$, we obtain with the help of Eqs. (46) and (47)

$$\lambda J(0, \omega^*) = \frac{2^6 \xi \beta^2 R^2}{\pi^{5/2}} \int_0^\infty dx_1 dx_2 \frac{\tilde{G}_0(x_1, x_2) \bar{G}(x_1, x_2)}{\omega^* - x_1^2 - x_2^2 + i\eta}. \quad (57)$$

Here we used $\omega^* = 2mR^2\omega$ and the dimensionless coupling constant ξ which can be written in terms of the scattering length a_0 according to Eq. (C11)

$$\xi = \frac{m\lambda}{4\pi^2\beta^3} = -\frac{1}{\sqrt{2\pi} + \frac{\pi}{\beta a_0}}. \quad (58)$$

Consequently, the potential is attractive for scattering length $a_0 > 0$ or $a_0 < -\sqrt{\pi/2}/\beta$ and repulsive otherwise. The potential range according to Eq. (C4) follows from Eq. (C11) as

$$r_0 = \frac{1}{\beta} \left(2\sqrt{\frac{2}{\pi}} + \frac{1}{a_0\beta} \right), \quad (59)$$

which shows that for negative scattering length we should have $a_0 < -\sqrt{\pi/2}/2\beta$ to render the potential range positive.

It is convenient to use the spectral representation following from Eq. (57)

$$\text{Re } \lambda J(0, \omega^*) = \frac{1}{\pi} \int_0^\infty d\omega \frac{\text{Im } \lambda J(0, \omega)}{\omega^* - \omega}$$

$$\text{Im } \lambda J(0, \omega^*) = -\frac{2^5 \xi \beta^2 R^2}{\pi^{3/2}} \times \int_0^{\sqrt{\omega^*}} dx_1 \frac{\tilde{G}_0(x_1, \sqrt{\omega^* - x_1^2}) \bar{G}(x_1, \sqrt{\omega^* - x_1^2})}{\sqrt{\omega^* - x_1^2}}. \quad (60)$$

The explicit analytical integrals \tilde{G}_0 and \bar{G} can be found in Appendix E.

The results are presented in Figs. 8–10. We compare the case with a cavity to the free two-particle scattering. The limit of contact potential $\beta \rightarrow \infty$ of the last chapter is plotted for comparison too. In Fig. 8 we have chosen a scattering length which does not allow the formation of bound states. The two-particle phase shift follows the general trend of the phase shift without cavity but shows characteristic oscillations which are visible in the cross section too. In Fig. 9 we chose such a scattering length that the free two-particle scattering has a bound state. While for the contact potential the repulsive opaque wall already destroys the bound state, the bound state survives in the finite-range potential. This means that the finite range enhances the correlations.

Decreasing the potential strength of the attractive two-particle scattering by a more negative scattering length the repulsive opaque wall will destroy also the bound state for the finite-range potential. In Fig. 10 we plot the limiting case where the bound state is just still realized.

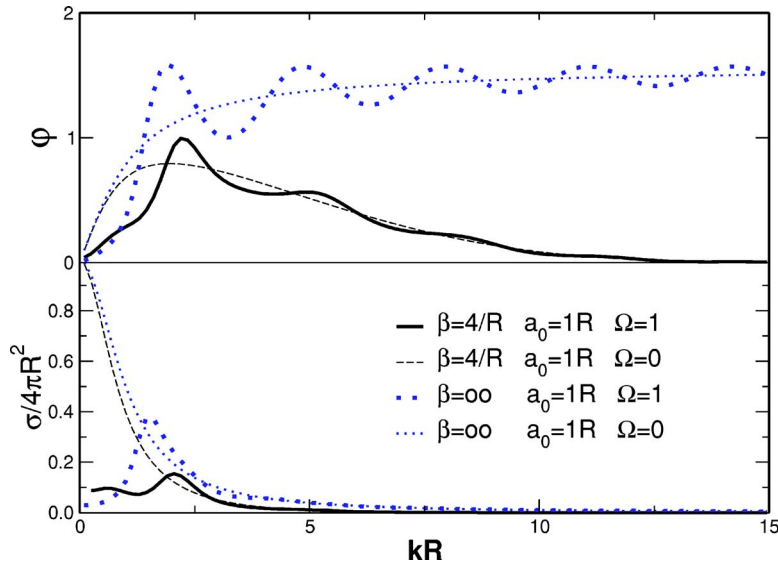


FIG. 8. (Color online) Two-particle phase shift (top) and cross section (bottom) in the presence of the cavity (thick lines) and without cavity (thin lines). The contact-potential case $\beta \rightarrow \infty$ (dotted lines) is compared with the finite-range case (solid and dashed lines). The scattering length is $a_0 = R$.

From the figures it is obvious that the finite-range potentials are more realistic than the contact potentials. For higher energies the phase shifts for the contact potential approach an artificial value of $\pi/2$ while the phase shifts for the finite-range potential approach zero as they should. For finite-range potentials also the cross section falls off faster than for contact potentials.

V. SUMMARY

We have investigated the coupled-channel problem of two particles interacting with themselves and with a cavity. We have chosen exactly solvable models for both the cavity as well as the two-particle potential in order to demonstrate the method. With the help of the single-particle wave function of the cavity, the two-particle problem is solved. For cavities with bound states the \mathcal{T} matrix is determined exactly. In the case of additional scattering states we restrict ourselves only to processes where the change of the center-of-mass momenta are negligible and present an approximate solution.

The influence of the cavity on the two-particle properties like scattering phase shift and bound states is investigated. We observe oscillations in the single-particle and two-particle phase shifts. While the oscillations in the single-particle phase shift are the standard resonances at the virtual levels of the cavity, the two-particle phase shift shows besides these oscillations also interferences which are visible in a splitting of the maxima in the cross section.

For repulsive opaque walls the scattering length must be negative but larger than a critical value in order that bound states remain. For attractive walls there is a specific range of negative wall parameters for which any negative scattering length will lead to bound states since both the cavity wall and the scattering length act attractively. In addition also positive scattering lengths will lead to bound states in this case provided the scattering length is larger than a critical value. For more attractive walls we could show that bound states are only possible for negative scattering lengths which are, however, limited by a negative critical value. The occurrence of such lower critical values is an unexpected effect of interference.

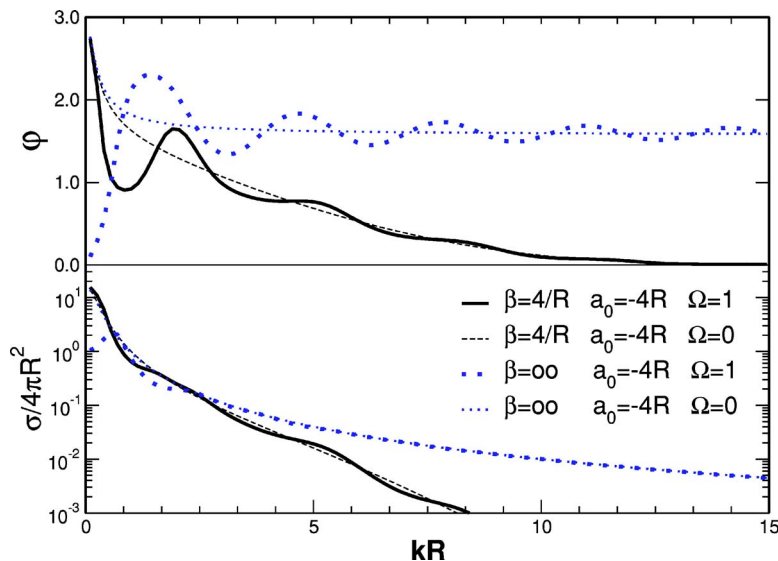


FIG. 9. (Color online) Same as Fig. 8, but for $a_0 = -4R$.

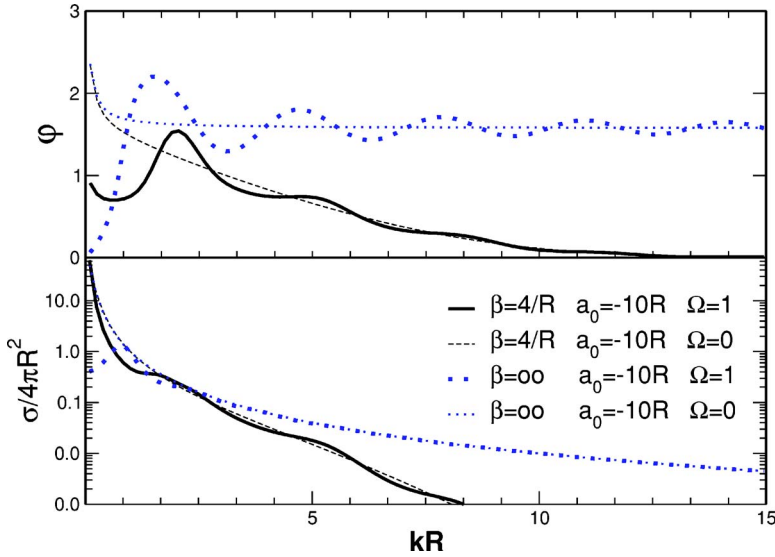


FIG. 10. (Color online) Same as Fig. 8, but for $a_0 = -10R$.

The model discussed here has the merit to be analytically solvable in all parts and serves as a toy model for more realistic situations. In particular, the finite cavity can be easily described by a more realistic wave function which enters the two-particle problem in such a way as worked out here. We intended to provide in this way a clear method which is also easily applicable to the case of two-particle scattering on any finite or more realistic structure, like crystals or amorphous structures. In this case one has to provide the single-particle wave functions, e.g., by an *ab initio* method and can use the method here to calculate the two-particle correlations explicitly.

The discussion here has been limited to the two-particle correlations for exploratory reasons. In a forthcoming work we will show how this method is applicable for the situation of many-particle correlations.

ACKNOWLEDGMENTS

This work has been supported by DAAD in Germany and by the research program MSM0021620834 of the Ministry of Education of Czech Republic. The discussions with Ingrid Rotter which have been of great value are gratefully acknowledged.

APPENDIX A: FORMULAS FROM COUPLED-CHANNEL SCATTERING THEORY

1. Many coupled channels

We consider a system consisting of i channels. Using the free propagator

$$\mathcal{G}_0(\omega) = \frac{1}{\omega - \mathcal{H}_0 + i\eta} \quad (\text{A1})$$

and the propagator including the interaction of the i th channel

$$\mathcal{G}_i(\omega) = \frac{1}{\omega - \mathcal{H}_i + i\eta}, \quad (\text{A2})$$

the Lippmann-Schwinger equation for the i th-channel propagator reads

$$\mathcal{G}_i(\omega) = \mathcal{G}_0(\omega) + \mathcal{G}_i(\omega)V_i\mathcal{G}_0(\omega) \quad (\text{A3})$$

corresponding to the i th-channel \mathcal{T} matrix

$$\mathcal{T}_i(\omega) = V_i + V_i\mathcal{G}_i(\omega)V_i. \quad (\text{A4})$$

The total \mathcal{T} matrix is described by the Lippmann-Schwinger equation with respect to the total potential $V = \sum_i V_i$ and can be written as a sum of auxiliary \mathcal{T} matrices

$$\mathcal{T}(\omega) = \sum_i V_i + \sum_i V_i\mathcal{G}_0(\omega)\mathcal{T}(\omega) = \sum_i \mathcal{T}'_i(\omega). \quad (\text{A5})$$

These auxiliary \mathcal{T} matrices are defined by

$$\mathcal{T}'_i = V_i + V_i\mathcal{G}_0\mathcal{T} \quad (\text{A6})$$

and can be rewritten as

$$\begin{aligned} \mathcal{T}'_i &= V_i + V_i\mathcal{G}_i\mathcal{T} - V_i\mathcal{G}_iV_i\mathcal{G}_0\mathcal{T} \\ &= V_i + V_i\mathcal{G}_iV_i\sum_{j \neq i} V_j\mathcal{G}_0V_j(1 + \mathcal{G}_0\mathcal{T}) \\ &= \mathcal{T}_i + \sum_{j \neq i} V_i\mathcal{G}_i\mathcal{T}'_j, \end{aligned} \quad (\text{A7})$$

where we used Eq. (A3) to write the first line and the definition (A6) to derive the last equality. Using further the identity $V_i\mathcal{G}_i = \mathcal{T}'_i\mathcal{G}_0$ the final form reads

$$\mathcal{T}'_i(\omega) = \mathcal{T}_i(\omega) + \sum_{j \neq i} \mathcal{T}_i(\omega)\mathcal{G}_0(\omega)\mathcal{T}'_j(\omega), \quad (\text{A8})$$

which shows how the single particle channel \mathcal{T} -matrices \mathcal{T}_i are coupled to yield the auxiliary \mathcal{T} matrices which add up to the total \mathcal{T} -matrix (A5).

2. Derivation of the Gell-Mann and Goldberger formula

In the case of only two channels the coupled \mathcal{T} matrices read

$$\begin{aligned} \mathcal{T} &= \mathcal{T}'_1 + \mathcal{T}'_2, \\ \mathcal{T}'_1 &= \mathcal{T}_1 + \mathcal{T}_1 \mathcal{G}_0 \mathcal{T}'_2, \\ \mathcal{T}'_2 &= \mathcal{T}_2 + \mathcal{T}_2 \mathcal{G}_0 \mathcal{T}'_1, \end{aligned} \quad (\text{A9})$$

and

$$\begin{aligned} \mathcal{T}_1 &= V_1 + V_1 \mathcal{G}_0 \mathcal{T}_1, \\ \mathcal{T}_2 &= V_2 + V_2 \mathcal{G}_0 \mathcal{T}_2. \end{aligned} \quad (\text{A10})$$

Introducing \mathcal{T}'_1 into \mathcal{T}'_2 from Eq. (A9) leads to

$$\mathcal{T}'_2 = \mathcal{T}_2(1 + \mathcal{G}_0 \mathcal{T}_1) + \mathcal{T}_2 \mathcal{G}_0 \mathcal{T}_1 \mathcal{G}_0 \mathcal{T}'_2 \quad (\text{A11})$$

with the help of which we define

$$\mathcal{T}_{ab} \equiv \mathcal{T}'_2(1 + \mathcal{G}_0 \mathcal{T}_1)^{-1} = \mathcal{T}_2 + \mathcal{T}_2 \mathcal{G}_0 \mathcal{T}_1 \mathcal{G}_0 \mathcal{T}_{ab}. \quad (\text{A12})$$

The total \mathcal{T} matrix from Eq. (A9) can then be written as

$$\mathcal{T} = \mathcal{T}_1 + (1 + \mathcal{T}_1 \mathcal{G}_0) \mathcal{T}'_2 = \mathcal{T}_1 + (1 + \mathcal{T}_1 \mathcal{G}_0) \mathcal{T}_{ab} (1 + \mathcal{G}_0 \mathcal{T}_1). \quad (\text{A13})$$

It remains to be shown that \mathcal{T}_{ab} is the \mathcal{T} matrix obeying a Lippman-Schwinger equation with the propagator \mathcal{G}_1 . For this purpose we use Eq. (A3)

$$-\mathcal{G}_0 = -\mathcal{G}_1 + \mathcal{G}_0 V_1 \mathcal{G}_1,$$

$$(1 - V_2 \mathcal{G}_1)^{-1} V_2 = (1 - \mathcal{T}_2 \mathcal{G}_0 V_1 \mathcal{G}_1)^{-1} \mathcal{T}_2, \quad (\text{A14})$$

where the second line follows from the first by trivial algebra. Now the right-hand side of Eq. (A14) is just the definition of \mathcal{T}_{ab} in Eq. (A12) using once more $\mathcal{T}_1 \mathcal{G}_0 = V_1 \mathcal{G}_1$. Therefore we see that from Eq. (A14) the Lippmann-Schwinger Eq. (3) for \mathcal{T}_{ab} follows:

$$\mathcal{T}_{ab} = V_2 + V_2 \mathcal{G}_1 \mathcal{T}_{ab}, \quad (\text{A15})$$

which completes the proof of the Gell-Mann and Goldberger formula (1) or Eq. (A13).

APPENDIX B: PROOF OF SEPARABILITY

A separable expansion is always possible for local interactions provided that the potential range is finite [$\mathcal{V}(r)=0$ for $r>R$]. We follow the presentation of Ref. 17 and start from the Lippmann-Schwinger equation with arbitrary energy ω (called off shell if $\omega \neq p^2/2m$),

$$|\psi\rangle = |p\rangle + \mathcal{G}_0 \mathcal{V} |\psi\rangle. \quad (\text{B1})$$

We expand the wave function inside the potential range,

$$|\psi\rangle = \sum_i |B_i\rangle \xi_i, \quad (\text{B2})$$

and multiply Eq. (B1) by $\langle B_j | \mathcal{V}$ from the left to obtain

$$\sum_i \langle B_j | \mathcal{V} | B_i \rangle \xi_i = \langle B_j | \mathcal{V} | p \rangle + \sum_i \langle B_j | \mathcal{V} \mathcal{G}_0 \mathcal{V} | B_i \rangle \xi_i. \quad (\text{B3})$$

Abbreviating $\mu_{ji} = \langle B_j | \mathcal{V} | B_i \rangle$, $\zeta_j = \langle B_j | \mathcal{V} | p \rangle$ and introducing the form factors

$$\langle g_j | = \langle B_j | \mathcal{V} \quad |g_i\rangle = \mathcal{V} |B_i\rangle \quad (\text{B4})$$

we can write Eq. (B3) as a matrix equation

$$\sum_i (\mu_{ji} - \langle g_j | \mathcal{G}_0 | g_i \rangle) \xi_i = \zeta_j \quad (\text{B5})$$

such that the expansion coefficients become

$$\xi_j = \sum_i \tau_{ij} \zeta_j \quad (\text{B6})$$

with $\tau_{ij}^{-1} = \mu_{ij} - \langle g_i | \mathcal{G}_0 | g_j \rangle$. Inserting Eq. (B6) into Eq. (B2) we have

$$\mathcal{V} |\psi\rangle = \sum_{ij} |g_i\rangle \tau_{ij} \langle g_j | p \rangle, \quad (\text{B7})$$

which shows that the effect of the potential on the scattering wave function can be expanded in separable form.

APPENDIX C: MODELS FOR FORM FACTORS OF SEPARABLE INTERACTION

For different parameterizations of the form factor g_q we can compute the unrestricted two-particle scattering expression of the \mathcal{T} -matrix (17)

$$\langle p_1 P | \mathcal{T}(\omega) | p_2 P' \rangle = \lambda \delta_{PP'} \frac{g_{p_1} g_{p_2}}{1 - \lambda J(P, \omega)}, \quad (\text{C1})$$

which is controlled by

$$\lambda J \left(P, \Omega = \omega - \frac{P^2}{4m} \right) = \frac{\lambda}{2\pi^2} \int_0^\infty dq q^2 \frac{g_q^2}{\Omega - \frac{q^2}{m} + i\eta}. \quad (\text{C2})$$

The phase shift is then given by Eq. (34)

$$\tan \varphi = \frac{\text{Im } \mathcal{T}}{\text{Re } \mathcal{T}} \Big|_{\Omega=p^2/2m} = \frac{\lambda J_I}{1 - \lambda J_R} \quad (\text{C3})$$

and the parameter of the potential can be linked to the scattering length a_0 and the range of the potential r_0 via the small wave-vector expansion

$$p \cot \varphi = \frac{1}{a_0} + \frac{r_0}{2} p^2 + \dots \quad (\text{C4})$$

The \mathcal{T} matrix possesses a pole, the bound state energy $\Omega = -E_b$ is given by

$$1 = \lambda J(-E_b). \quad (\text{C5})$$

It will be useful to use a dimensionless scaled potential strength $\xi = m\lambda/4\pi^2\beta^3$ in the following.

1. Exponential function

As a first example we choose a form factor

$$g_p = \beta^{-2} e^{-p^2/4\beta^2} \quad (\text{C6})$$

and obtain for $\Omega > 0$ with $y' = \sqrt{m\Omega/2\beta^2}$

$$\lambda J(\Omega) = -\xi \sqrt{2\pi} (1 + F(y') + i\sqrt{\pi} y' e^{-y'^2}) \quad (\text{C7})$$

and the Fred-Conte function

$$F(z) = \frac{2z^2}{\sqrt{\pi}} \int_0^\infty dx \frac{e^{-x^2}}{x^2 - z^2}. \quad (\text{C8})$$

The scattering phase shift becomes

$$\tan \varphi = -\sqrt{2\pi} \xi \frac{y' e^{-y'^2}}{1 + \sqrt{2\pi} \xi [1 + F(y')]} \quad (\text{C9})$$

from which we obtain the expansion

$$p \cot \varphi = -\beta \frac{\sqrt{2\pi} \xi + 1}{\pi \xi} + \frac{\sqrt{2\pi} \xi - 1}{2\beta \pi \xi} p^2 \quad (\text{C10})$$

and comparing with Eq. (C4) we can link the potential parameter to the scattering length and the potential range as

$$a_0 = -\frac{1}{\beta} \frac{1}{\frac{1}{\pi \xi} + \sqrt{\frac{2}{\pi}}}$$

$$r_0 = \frac{1}{\beta} \left(\sqrt{\frac{2}{\pi}} - \frac{1}{\pi \xi} \right). \quad (\text{C11})$$

For negative energies $\Omega = -E_b < 0$ we obtain with $y = -iy' = \sqrt{mE_b}/2\beta^2$

$$\lambda J(-E_b) = -\xi \sqrt{2\pi} (1 - \sqrt{\pi} y e^{y^2} \operatorname{erfc}(y)) \quad (\text{C12})$$

such that the condition for bound states becomes

$$1 + \xi \sqrt{2\pi} (1 - \sqrt{\pi} y e^{y^2} \operatorname{erfc}(y)) = 0 \quad (\text{C13})$$

from which follows that only for $\xi < 0$ there can be bound states. Rewriting it we get

$$|\xi| \sqrt{2\pi} = \frac{1}{1 - \sqrt{\pi} y e^{y^2} \operatorname{erfc}(y)}. \quad (\text{C14})$$

The right-hand side is a monotonically increasing function of y starting from 1 for $y=0$. Therefore, bound states are only possible if

$$\xi < -\frac{1}{\sqrt{2\pi}}. \quad (\text{C15})$$

2. Step function

As a second example, the form factor is assumed to be a step function cutoff in real space $g_r = \Theta(R-r)/4\pi\hbar^2 r$ from which we have

$$g_p = \frac{1 - \cos pR/\hbar}{p^2}. \quad (\text{C16})$$

For the scattering case $\Omega = p^2/m > 0$ we obtain

$$\lambda J = \xi \left(\frac{\beta}{p} \right)^3 \left[\frac{p}{\beta} + \sin \frac{p}{\beta} \left(\cos \frac{p}{\beta} - 2 \right) - i \left(1 - \cos \frac{p}{\beta} \right)^2 \right] \quad (\text{C17})$$

from which the relation to the scattering length and the potential range follows:

$$a_0 = \frac{1}{4\beta} \left(\frac{1}{3} + \frac{1}{\xi} \right)^{-1}$$

$$r_0 = \frac{2}{3\beta} \left(\frac{11}{15} - \frac{2}{\xi} \right). \quad (\text{C18})$$

The condition of bound states, for $\Omega = -E_b$, reads

$$\lambda J = -\frac{\xi}{4\sqrt{2}y^3} (2\sqrt{2}y + 1 - (e^{-\sqrt{2}y} - 2)^2) \quad (\text{C19})$$

so that we can obtain bound states if

$$-\frac{1}{\xi} = \frac{2\sqrt{2}y + 1 - (e^{-\sqrt{2}y} - 2)^2}{4\sqrt{2}y^3} \quad (\text{C20})$$

and since the right-hand side is a monotonically decreasing function starting from 1/3 at $y=0$ we obtain the condition for bound states

$$\xi < -3. \quad (\text{C21})$$

3. Yamaguchi form factor

The traditional form factor is

$$g_p = \frac{1}{\beta^2 + p^2}. \quad (\text{C22})$$

For $\Omega = p^2/m > 0$ we obtain

$$\lambda J = \xi \beta^2 \pi \frac{p^2 - \beta^2 - 2ip\beta}{2(\beta^2 + p^2)^2} \quad (\text{C23})$$

and the scattering phase shift becomes

$$\cot \varphi = \frac{(p^2 + \beta^2)^2}{-\pi \xi p \beta^3} + \frac{p^2 - \beta^2}{2\beta p}. \quad (\text{C24})$$

Expanding in p and comparing with Eq. (A3) we determine the potential parameters from

$$a_0 = -\frac{2}{\beta \left(\frac{2}{\pi \xi} + 1 \right)}, \quad (\text{C25})$$

$$r_0 = \frac{1}{\beta} \left(1 - \frac{4}{\xi \pi} \right). \quad (\text{C26})$$

The case of $\Omega = -E_b$ leads to

$$\lambda J(-E_b) = -\frac{\pi\xi}{2(1+\sqrt{2}y)^2} \quad (\text{C27})$$

such that we obtain bound states if

$$\xi = -\frac{2(1+\sqrt{2}y)^2}{\pi}. \quad (\text{C28})$$

Therefore the condition for bound states is

$$\xi < -\frac{2}{\pi}. \quad (\text{C29})$$

APPENDIX D: INTEGRAL OF EQ. (50)

The integral (50) can be evaluated analytically. To this end we rewrite Eq. (50) as

$$F_\Omega(z) = \frac{\Omega}{\pi} \int_0^1 dc (\delta_{c,1} + \Omega) \int_{-\infty}^{\infty} dy \frac{\sin cy}{y-2z} \frac{1}{n(y)} \quad (\text{D1})$$

with

$$n(y) = 1 + 2\frac{\Omega}{y} \sin y + 2\frac{\Omega^2}{y^2} (1 - \cos y). \quad (\text{D2})$$

We use the representation of the principal value $1/y = \frac{1}{2} [1/(y-i\eta) + 1/(y+i\eta)]$ and obtain

$$F = \int_0^1 dc (\Omega \delta_{c,1} + \Omega^2) \text{Re} \left(\frac{e^{2izc}}{n(2z)} + 2 \sum_{\nu} \frac{e^{icy_{\nu}}}{y_{\nu} - 2z} \frac{1}{n'(y_{\nu})} \right) \\ = \frac{\Omega \cos 2z + \Omega^2 \frac{\sin 2z}{2z}}{n(2z)} + 2 \sum_{\nu} \frac{\Omega e^{iy_{\nu}} + \frac{\Omega^2}{iy_{\nu}} (e^{iy_{\nu}} - 1)}{y_{\nu} - 2z} \frac{1}{n'(y_{\nu})}. \quad (\text{D3})$$

The values y_{ν} represent the complex zeros of $n(y)$. Setting $y_{\nu} = \mp 2it_{\nu}$ these zeros obey

$$\tanh t_{\nu} = -\frac{t_{\nu}}{t_{\nu} + \Omega}. \quad (\text{D4})$$

Observing that $1/n(2z) = A_z^2$ and straightforward algebra using Eq. (D4) leads to the final representation of the integral as

$$F_\Omega(z) = \Omega \left(\cos 2z + \Omega \frac{\sin 2z}{2z} \right) A_z^2 + 2 \sum_{\nu} \frac{t_{\nu}}{t_{\nu} + iz} \frac{2t_{\nu} + \Omega}{1 + \Omega + 2t_{\nu}}. \quad (\text{D5})$$

The special value required for Eq. (55) reads

$$F_\Omega(0) = \frac{\Omega}{\Omega + 1} + 2 \sum_{\nu} \frac{2t_{\nu} + \Omega}{1 + \Omega + 2t_{\nu}}, \quad (\text{D6})$$

where for $\Omega > 0$ Eq. (D4) has no solution and therefore the last sum in Eqs. (D5) and (D6) is absent.

Another straightforward rewriting yields the relation

$$F_\Omega(ib) - F_\Omega(0) = -b + \frac{2b^2}{\pi} \int_0^{\infty} \frac{dx}{x^2 + b^2} A_x^2 \quad (\text{D7})$$

which proves $F_\Omega(ib) + b \geq F_\Omega(0)$ used in the discussion following Eq. (54) where $b = R\sqrt{mE_b}$.

APPENDIX E: OTHER OCCURRING INTEGRALS

Here we calculate the integrals appearing in Sec. IV B.

1. $G_{n_1 n_2}(\mathbf{0})$

The first integral we consider is

$$G_{n_1 n_2}(\mathbf{0}) = \int d\mathbf{r} G_{n_1 n_2}(\mathbf{r}) = \int \frac{d\mathbf{q}}{(2\pi)^3} g_{\mathbf{q}} \Psi_{\mathbf{k}_1}(\mathbf{q}) \Psi_{\mathbf{k}_2}(-\mathbf{q}). \quad (\text{E1})$$

It is convenient here to use the wave function in momentum space. We obtain for the cavity model (5)

$$\chi_k(q) = -4\pi c R \left(\frac{\Omega \sin(qR) \sin(x + \phi)}{q^2 R^2 - x^2} - \frac{\pi \cos \phi}{2} \delta(qR - x) \right) \quad (\text{E2})$$

with $x = kR$ or for the three-dimensional wave function

$$\Psi_k(\mathbf{q}) = -cR^2 \left[\frac{4\pi\Omega \sin(qR) \sin(x + \phi)}{x(q^2 R^2 - x^2)} - x(2\pi)^3 \delta(\mathbf{qR} - \mathbf{x}) \cos \phi \right]. \quad (\text{E3})$$

Changing variables $y = qR$ in Eq. (E1) we obtain

$$G_{n_1 n_2}(\mathbf{0}) = \frac{8Rc^2}{\beta^2} \tilde{G}_0(\mathbf{x}_1, \mathbf{x}_2) \quad (\text{E4})$$

and using the exponential form factor of Appendix C 1, we obtain with $\gamma = 2R\beta$

$$\tilde{G}_0(\mathbf{x}_1, \mathbf{x}_2) = \int_0^{\infty} dy e^{-y^2/\gamma^2} \frac{\Omega^2 \sin^2 y \sin(x_1 + \phi_1) \sin(x_2 + \phi_2)}{(y^2 - x_1^2)(y^2 - x_2^2)} \\ - \frac{\Omega\pi}{2(x_1^2 - x_2^2)} (e^{-x_1^2/\gamma^2} \sin x_1 \sin(x_2 + \phi_2) \cos \phi_1 \\ + e^{-x_2^2/\gamma^2} \sin x_2 \sin(x_1 + \phi_1) \cos \phi_2) \\ + \pi^3 x_1^2 \delta(\mathbf{x}_1 + \mathbf{x}_2) \cos \phi_1^2 e^{-x_1^2/\gamma^2}. \quad (\text{E5})$$

The remaining integral can be written as

$$\int_0^{\infty} \frac{e^{-y^2/\gamma^2} \sin^2 y}{(y^2 - x_1^2)(y^2 - x_2^2)} = \begin{cases} \frac{I_\gamma(x_1^2) - I_\gamma(x_2^2)}{x_1^2 - x_2^2} & x_1 \neq x_2 \\ \frac{1}{2x_1} \frac{\partial}{\partial x_1} I_\gamma(x_1^2) & x_1 = x_2 \end{cases} \quad (\text{E6})$$

with

$$\begin{aligned}
I_\gamma(x^2) &= \int_0^\infty dy \frac{e^{-y^2/\gamma^2} \sin y^2}{y^2 - x^2} \\
&= \frac{1}{4x} \int_{-\infty}^\infty dt e^{-t^2} \frac{1 - \cos 2\gamma t}{t - x/\gamma} \\
&= \frac{1}{4x} [-\pi \operatorname{Im} W(x/\gamma) - f(2\gamma, x/\gamma)]. \quad (\text{E7})
\end{aligned}$$

Here we used the standard integral representation of the complex error function for $W(z) = e^{-z^2} \operatorname{erfc}(-iz)$ and abbreviated

$$f(a, b) = \int_{-\infty}^\infty dt \frac{e^{-t^2} \cos(at)}{t - b}. \quad (\text{E8})$$

This integral can be solved analytically. To this end we observe that

$$f(0, b) = -\pi \operatorname{Im} W(b) \quad (\text{E9})$$

$$\left. \frac{\partial}{\partial a} f(a, b) \right|_{a=0} = 0 \quad (\text{E10})$$

and find a differential equation from Eq. (E8)

$$\partial_a^2 f(a, b) + b^2 f(a, b) = -b \sqrt{\pi} e^{-a^2/4}. \quad (\text{E11})$$

This linear inhomogeneous differential equation with constant coefficients can be solved straightforwardly and with the boundary conditions (E10) we obtain finally

$$f(a, b) = \pi e^{-b^2} \operatorname{Im} e^{-iab} \operatorname{erf}\left(\frac{a}{2} - ib\right). \quad (\text{E12})$$

2. $\int d\mathbf{p} G_{n_1 n_2}(\mathbf{p})$

The second integral used in Eq. (56) is conveniently expressed by the wave functions in spatial representation

$$\int \frac{d\mathbf{p}}{(2\pi)^3} G_{n_1 n_2}(\mathbf{p}) = \int d\mathbf{r} g_r \Psi_{\mathbf{k}_1}(\mathbf{r}/2) \Psi_{\mathbf{k}_2}(-\mathbf{r}/2) \quad (\text{E13})$$

where we use the Fourier transform of Eq. (E3)

$$\Psi_{\mathbf{k}}(\mathbf{r}) = cke^{i\mathbf{k}\mathbf{r}} \cos \phi + \frac{c \sin \phi}{r} \begin{cases} \cot x \sin(kr) & r < R \\ \cos(kr) & r > R \end{cases}. \quad (\text{E14})$$

For the exponential form factor of Appendix C 1 the integrals in Eq. (E13) becomes

$$\int \frac{d\mathbf{p}}{(2\pi)^3} G_{n_1 n_2}(\mathbf{p}) = \frac{32R\beta c^2}{\sqrt{\pi}} \bar{G}(x_1, x_2). \quad (\text{E15})$$

The integral (E5) contains a term $\sim \delta(\mathbf{x}_1 + \mathbf{x}_2)$ and will be multiplied with Eq. (E13) as part of the integrand in Eq. (57). Therefore special care is needed to evaluate Eq. (E13) for the diagonal case $\mathbf{x}_1 = -\mathbf{x}_2$. We split therefore $\bar{G}(x_1, x_2) = \bar{G}'(x_1, x_2) + \bar{G}''(x_1)$ where we use for the first term the radial component of Eq. (E14) and summarize in the second part the difference of the angular integral over the wave functions and the radial one. This difference vanishes except for the case $\mathbf{x}_1 = -\mathbf{x}_2$.

Changing variables $y = r/R$ in Eq. (E13) we obtain for the regular part \bar{G}'

$$\begin{aligned}
\bar{G}'(x_1, x_2) &= A_{x_1}^2 A_{x_2}^2 \int_0^1 dy e^{-y^2/\gamma^2} \sin x_1 y \sin x_2 y \\
&\quad + \int_1^\infty dy e^{-y^2/\gamma^2} \sin(x_1 y + \phi_1) \sin(x_2 y + \phi_2), \quad (\text{E16})
\end{aligned}$$

which are trivial integrals. The irregular part \bar{G}'' is now the difference between the angular averaging of the vectorial part of the wave functions $\sim k_1 r \sin k_1 r$ and the expression of the radial part of the wave function $\sim \sin^2 k_1 r$ since the latter is already absorbed in the regular part. We obtain

$$\bar{G}''(x_1) = \cos^2 \phi_1 \int_0^\infty dy e^{-y^2/\gamma^2} [x_1 y \sin(2x_1 y) - (\sin x_1 y)^2], \quad (\text{E17})$$

which again is a trivial integral.

¹T. Fujisawa, D. G. Austing, Y. Tokura, Y. Hirayama, and S. Tarucha, *Nature (London)* **419**, 278 (2002).

²C. Schüller, K. B. Broocks, C. Heyn, and D. Heitmann, *Phys. Rev. B* **65**, 081301(R) (2002).

³N. A. Fromer, C. Schüller, C. W. Lai, D. S. Chemla, I. E. Perakis, D. Driscoll, and A. C. Gossard, *Phys. Rev. B* **66**, 205314 (2002).

⁴M. A. Reed, J. N. Randall, R. J. Aggarwal, R. J. Matyi, T. M. Moore, and A. E. Wetsel, *Phys. Rev. Lett.* **60**, 535 (1988).

⁵E. B. Foxman, P. L. McEuen, U. Meirav, N. S. Wingreen, Y. Meir, P. A. Belk, N. R. Belk, M. A. Kastner, and S. J. Wind, *Phys. Rev. B* **47**, R10020 (1993).

⁶J. Kyriakidis, M. Pioro-Ladriere, M. Ciorga, A. S. Sachrajda, and P. Hawrylak, *Phys. Rev. B* **66**, 035320 (2002).

⁷J. R. Taylor, *Scattering Theory of Nonrelativistic Collisions* (Wiley, New York, 1972).

⁸P. Beregi, I. Lovas, and J. Revai, *Ann. Phys.* **61**, 57 (1970).

⁹P. Beregi and I. Lovas, *Z. Phys.* **241**, 410 (1971).

¹⁰P. Beregi, *Z. Phys.* **257**, 440 (1972).

¹¹M. Gell-Mann and M. L. Goldberger, *Phys. Rev.* **91**, 398 (1953).

¹²W. R. Gibbs, *Phys. Rev. C* **10**, 2166 (1974).

¹³L. Canton and G. H. Rawitscher, *J. Phys. G* **17**, 429 (1991).

¹⁴G. H. Rawitscher and L. Canton, *Phys. Rev. C* **44**, 60 (1991).

¹⁵S. Flügge, *Practical Quantum Mechanics* (Springer, Berlin,

- 1994).
- ¹⁶Y. Koike, *Prog. Theor. Phys.* **87**, 775 (1992).
- ¹⁷Y. Koike, W. C. Parke, L. C. Maximon, and D. R. Lehman, *Few-Body Syst.* **23**, 53 (1997).
- ¹⁸N. H. Kwong and H. S. Köhler, *Phys. Rev. C* **55**, 1650 (1997).
- ¹⁹M. Schmidt, T. Janke, and R. Redmer, *Contrib. Plasma Phys.* **29**, 431 (1989).
- ²⁰M. Schmidt, G. Röpke, and H. Schulz, *Ann. Phys. (N.Y.)* **202**, 57 (1990).
- ²¹T. Alm, G. Röpke, and M. Schmidt, *Phys. Rev. C* **50**, 31 (1994).
- ²²K. Morawetz and G. Röpke, *Z. Phys. A* **355**, 287 (1996).
- ²³K. Morawetz, *Phys. Rev. B* **66**, 172508 (2002).
- ²⁴Y. Yamaguchi, *Phys. Rev.* **95**, 1628 (1954).
- ²⁵E. M. Lifschitz and L. P. Pitaevsky, *Statistical Physics II* (Akademie Verlag, Berlin, 1989).
- ²⁶We follow here the convention of Ref. 28 which has an opposite sign compared to Ref. 15.
- ²⁷Please note that for positive scattering lengths there is an even number of bound states and for negative scattering lengths there is an odd number (Ref. 28). Only for contact potentials the sign of the coupling strength follows the sign of the scattering length.
- ²⁸M. L. Goldberger and K. M. Watson, *Collision Theory* (Wiley, New York, 1964).